

Injected-Hot-Electron Transport in GaAs

A. F. J. Levi

AT&T Bell Laboratories, Murray Hill, New Jersey 07974

J. R. Hayes

Bell Communications Research, Murray Hill, New Jersey 07974

and

P. M. Platzman and W. Wiegmann

AT&T Bell Laboratories, Murray Hill, New Jersey 07974

(Received 3 July 1985)

Using the new experimental technique of hot-electron spectroscopy we have, for the first time, observed electrons in extreme nonequilibrium. When the transit-region width is comparable to the calculated hot-electron mean free path, two peaks are observed in the measured spectrum. The high-energy peak corresponds to quasiballistic electrons suffering few, if any, collisions in the transit region. The low-energy peak is due to excitation of the Fermi sea by the injected hot electrons.

PACS numbers: 72.20.Jv

Modern fabrication techniques allow one to construct semiconductor devices with dimensions comparable to the mean free path of charge carriers. Transport in such systems is nondiffusive in character, being determined by only a few scattering events. In this regime charge carriers may attain a nonthermal "hot" energy distribution in which they are in equilibrium neither with the lattice nor with themselves. Of particular interest is the case of charge carriers injected into a semiconductor with energy significantly in excess of the Fermi energy, as it is in this regime that one may gain insight into the physics of hot-electron transport. In this Letter we present new experimental results on the dynamics of injected, nonequilibrium, electrons in GaAs and we develop a theory with which to interpret the measurements.

New experimental information on hot electrons in GaAs was obtained by use of the technique of hot-electron spectroscopy.^{1,2} This technique utilizes two bulk triangular potential barriers placed in a single crystal of GaAs grown by molecular-beam epitaxy. Each triangular barrier is made by the placement of an approximately 100-Å-thick p^+ (Be impurity) layer in a region of low carrier concentration ($< 1 \times 10^{-15} \text{ cm}^{-3}$) bounded on either side by n^+ (Si impurity) layers.³ In an ideal case (see the energy-band diagram in the inset of Fig. 1) hot electrons are injected over one barrier into a short transit region where scattering takes place. A second triangular barrier placed at the other end of the transit region is used as a hot-electron analyzer. The analyzer energy may be varied by application of a bias voltage between the transit region at ground potential and the collector arm of the analyzer. In this way spectroscopic information on the current flow across the barrier may be measured. The derivative of this current with respect to the analyzer barrier

energy is proportional to $n(p_{\perp})$, the number of extra electrons with sufficient momentum perpendicular to the analyzer barrier, p_{\perp} , to just surmount the barrier.² Measurements were performed with the sample at a temperature of 4.2 K to avoid the possibility of any thermal smearing effects.

In a previous Letter we outlined the experimental technique of hot-electron spectroscopy² and obtained spectra for GaAs samples having a degenerate-electron concentration of $1 \times 10^{18} \text{ cm}^{-3}$ and transit-region widths greater than 1200 Å. The spectra had a broad peak at low energies (high voltage biases) with no evidence of the initial injected distribution. In order to investigate the extreme nonequilibrium limit the transit region was narrowed so that the injected distribution could be probed. In Fig. 1 a typical hot-electron spectrum is shown for a sample having a 650-Å-wide transit region, carrier concentration $n = 1 \times 10^{18} \text{ cm}^{-3}$, and an injection energy of 250 meV. The spectrum shown in Fig. 1 has two main features, a broad peak at high barrier energy ($\sim 0.1\text{-V}$ bias) and a sharp peak at low barrier energy ($\sim 0.7\text{-V}$ bias) near the Fermi energy, E_F , of the transit region. The peak at low energies ($\sim 0.7\text{-V}$ bias) is seen in all samples with varying transit-region widths. The high-energy peak, close to the injection energy, is only detectable in samples having narrow (less than ~ 850 Å) transit regions. We shall for the moment assign this high-energy peak to quasiballistic electrons, i.e., high-energy electrons having suffered few if any elastic or inelastic collisions. In order to give this assignment a sound foundation and to interpret the low-energy feature in the spectrum it is necessary to develop a theory which describes the dynamics of injected hot electrons.

When the injected electron is inelastically scattered it loses energy $\hbar\omega$ and changes momentum by $\hbar q$. In

the Born approximation the differential rate is given by⁴

$$dR_{\text{inelastic}} = \frac{8\pi e^2}{\hbar q^2} S(q, \omega) \frac{d^3 q}{(2\pi)^3}, \quad (1)$$

where

$$S(q, \omega) = -\text{Im}[1/\epsilon(q, \omega)]. \quad (2)$$

The frequency- and wave-vector-dependent dielectric function $\epsilon(q, \omega)$ may be written as

$$\epsilon(q, \omega) = \epsilon_\infty (\omega^2 - \omega_{\text{LO}}^2) / (\omega^2 - \omega_{\text{TO}}^2) + \chi(q, \omega), \quad (3)$$

where ω_{LO} and ω_{TO} are the longitudinal- and transverse-optical phonon frequencies, respectively,

$$\chi_0(q, \omega) = \frac{\xi}{x^3} \left\{ 2x + \left[1 - \frac{1}{4} \left(x - \frac{y}{x} \right)^2 \right] \ln \left[\frac{y - x(x+2)}{y - x(x-2)} \right] + \left[1 - \frac{1}{4} \left(x + \frac{y}{x} \right)^2 \right] \ln \left[\frac{-y - x(x+2)}{-y - x(x-2)} \right] \right\}, \quad (4)$$

in which

$$\xi = \frac{m_e}{2} \left(\frac{e}{\pi \hbar} \right)^2 \left(\frac{8\pi}{3n} \right)^{1/3},$$

$x = q/k_F$, and $y = \hbar\omega/E_F$, where k_F is the Fermi wave vector.

$S(q, \omega)$ in Eq. (1) contains an energy-conserving δ function. Assuming that the injected electron has momentum p and energy $p^2/2m_e$, we can integrate $dR_{\text{inelastic}}$ over all q consistent with momentum and en-

ergy conservation to obtain a total inelastic rate $1/\tau$ for an electron of energy $p^2/2m_e$. In Fig. 2 we plot the total inelastic scattering rate $1/\tau$ as a function of the hot-electron energy measured from the bottom of the conduction band for several different carrier densities in GaAs. We note that our definition of total inelastic scattering rate does not weight $1/\tau$ with the energy loss. As can be seen the scattering rates are, as expected, zero below the Fermi energy for a finite carrier concentration and zero below $\hbar\omega_{\text{LO}}$ for $n = 0$.

At density $n = 1 \times 10^{18} \text{ cm}^{-3}$ the inelastic scattering rate increases, attaining a maximum value of approximately $2 \times 10^{13} \text{ s}^{-1}$ at incident electron energies of around 250 meV. The velocity of such an electron is $\sim 1 \times 10^8 \text{ cm s}^{-1}$ giving a mean free path of 500 Å, an

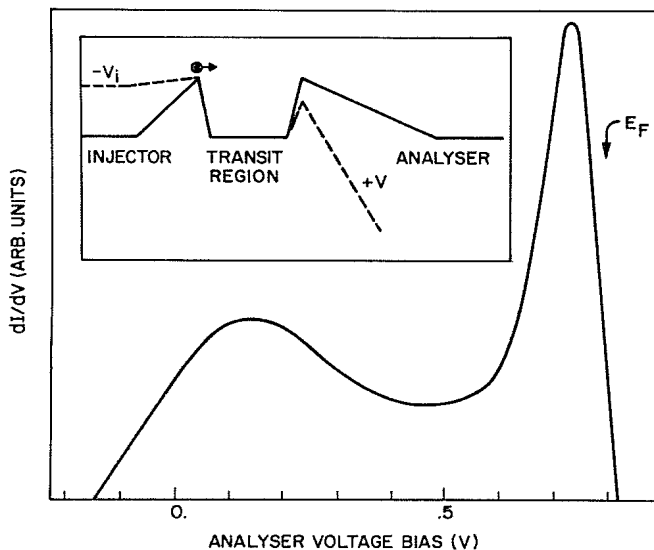


FIG. 1. Hot-electron spectrum for a sample having a 650-Å transit region and $n = 1 \times 10^{18} \text{ cm}^{-3}$. The Fermi energy, E_F , is indicated. Inset: schematic of the conduction-band edge of the hot-electron injector, the transit region, and the hot-electron analyzer. The broken lines indicate the conduction-band edge of the structure when biased with voltage $-V_i$ at the injector and $+V$ at the analyzer.

ergy conservation to obtain a total inelastic rate $1/\tau$ for an electron of energy $p^2/2m_e$. In Fig. 2 we plot the total inelastic scattering rate $1/\tau$ as a function of the hot-electron energy measured from the bottom of the conduction band for several different carrier densities in GaAs. We note that our definition of total inelastic scattering rate does not weight $1/\tau$ with the energy loss. As can be seen the scattering rates are, as expected, zero below the Fermi energy for a finite carrier concentration and zero below $\hbar\omega_{\text{LO}}$ for $n = 0$.

At density $n = 1 \times 10^{18} \text{ cm}^{-3}$ the inelastic scattering rate increases, attaining a maximum value of approximately $2 \times 10^{13} \text{ s}^{-1}$ at incident electron energies of around 250 meV. The velocity of such an electron is $\sim 1 \times 10^8 \text{ cm s}^{-1}$ giving a mean free path of 500 Å, an

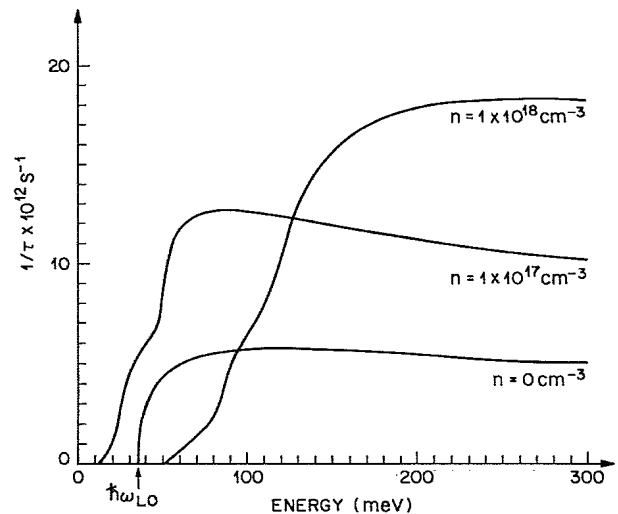


FIG. 2. Total inelastic scattering rate as a function of hot-electron energy measured from the bottom of the conduction band for the indicated carrier densities in GaAs.

average scattering angle $\theta_{av} \sim 30^\circ$, and an average energy loss of ~ 40 meV. At incident electron energies greater than 300 meV complications associated with intervalley scattering and with details of Bloch wave functions arise because of the subsidiary L minimum⁷ in GaAs. We therefore restrict our calculation to energies below 300 meV.

In addition, there is an elastic contribution to the scattering rate from donor ions screened by conduction electrons. Elastic scattering is specified by momentum transfer $q = 2k_i \sin(\theta/2)$ where θ is the scattering angle. In the Born approximation the differential rate is

$$dR_{\text{elastic}} = \frac{2\pi n_i m_e e^4}{\hbar^3 k_i^3} \frac{\eta d\eta}{[\eta^2 \epsilon(2k_i, \eta, 0)]^2}, \quad (5)$$

where n_i is the density of ionized impurities ($n_i = n$) and $\eta = \sin(\theta/2)$. Evaluation of the total rate gives a mean free path of around 1300 Å for electron density $n = 1 \times 10^{18} \text{ cm}^{-3}$ and hot-electron energy $E_i = 250$ meV. We note that our definition of total elastic scattering rate does not weight the rate with scattering angle. However, the major contribution to the elastic rate comes from small-angle scattering (average scattering angle $\theta_{av} \sim 20^\circ$ for $E_i = 250$ meV). We therefore conclude that elastic scattering at these densities does not play a dominant role, the mean free path of hot electrons essentially being determined by inelastic scattering events.

Since the transit-region width for the data shown in Fig. 1 is comparable to the calculated hot-electron mean free path it is apparent that our initial assignment of this peak is correct and it arises from quasiballistic electrons. The broadness of this high-energy peak may, in part, be due to fluctuations in the analyzer barrier energy caused by the random position of p -type impurities used to form the planar triangular barrier. This could be overcome once compositionally graded AlGaAs barriers of sufficient quality can be fabricated. With use of Eq. (1), it can be shown that the low-energy feature in Fig. 1 arises because electrons are excited from the Fermi sea by the injected hot electrons. While the detailed shape of the low-energy peak in the spectrum can be calculated by use of the single-scattering Born approximation we do not present the results of such a calculation here. However, if multiple-scattering events are included then we must take into account the important role, at these low energies, of elastic scattering and the modification of the inelastic scattering rate due to the exchange interaction between excited electrons and the Fermi sea.

In addition, it should be noted that if such detailed analysis is undertaken, the role played by multiple quantum reflections at the injector and analyzer barriers, in shaping the spectra, must be considered.

In conclusion, we have measured hot-electron spectra of GaAs samples having narrow transit-region widths. The measured spectra differ dramatically from previous spectroscopic studies of hot electrons which have exclusively used photoluminescence.⁸ Such studies are invariably interpreted in terms of an effective electron temperature inferred from an assumed Maxwell-Boltzmann distribution. Although deviations from the effective-electron-temperature concept have been commented on before, we have observed a double-peaked, extreme nonequilibrium, electron distribution highlighting the inadequacy of the temperature concept. Our measured spectra show a peak at high energies, close to injection energy, that we attribute to quasiballistic electrons. A second peak observed at low energies we identify with excitations of the Fermi sea. Finally, our theory of injected-hot-electron transport in GaAs indicates that inelastic electron scattering dominates the transport process at the carrier concentrations of interest.

We wish to thank S. J. Allen, S. L. McCall, and H. L. Stormer for many useful discussions, and T. Uchida for technical assistance.

¹J. R. Hayes, A. F. J. Levi, and W. Weigmann, *Electron. Lett.* **20**, 851 (1984).

²J. R. Hayes, A. F. J. Levi, and W. Weigmann, *Phys. Rev. Lett.* **54**, 1570 (1985).

³R. J. Malik, K. Board, C. E. C. Wood, L. F. Eastman, T. R. AuCoin, and R. L. Ross, *Electron. Lett.* **16**, 837 (1980).

⁴D. Pines and P. Nozières, *The Theory of Quantum Liquids* (Benjamin, New York, 1966).

⁵M. E. Kim, A. Das, and S. D. Senturia, *Phys. Rev. B* **18**, 6890 (1978).

⁶In other cases where we cannot replace $\chi(q, \omega)$ by $\chi_0(q, \omega)$, for example, GaAs in a strong magnetic field, we can think of using hot-electron spectroscopy of thin samples to obtain information on $\chi(q, \omega)$.

⁷H. C. Casey and M. B. Panish, *Heterostructure Lasers, Part A: Fundamental Principles* (Academic, London, 1978), p. 193.

⁸J. Shah and R. F. Leheny, in *Semiconductors Probed by Ultrafast Laser Spectroscopy*, edited by R. R. Alfano (Academic, London, 1984), pp. 45-76.